A rigorous lower bound for the stability regions of the quadratic map

Warwick Tucker and Daniel Wilczak
Department of Mathematics
University of Bergen
Johannes Brunsgate 12, 5008 Bergen, Norway
`first.last@math.uib.no`

July 6, 2009

Abstract

We establish a lower bound on the measure of the set of stable parameters a for the quadratic map $Q_a(x) = ax(1-x)$. For these parameters, we prove that Q_a either has a single stable periodic orbit or a period-doubling bifurcation. From this result, we also obtain a non-trivial upper bound on the set of stochastic parameters for Q_a.

Keywords: Quadratic map, periodic orbit, period doubling bifurcation, interval analysis.
2000 MSC: Primary: 37E05; Secondary: 34–04, 37G15, 65G20.

1 Introduction

The quadratic map (often referred to as the *logistic map*)

$$Q_a\colon [0,1] \to [0,1] \qquad x \mapsto ax(1-x), \tag{1}$$

is arguably the most studied discrete dynamical system. Beginning with the famous article by Robert May [Ma76], the intricate properties of this dynamical system have gradually been revealed, see e.g. [CE80], [Ep85], [Fe79], [La82], [Ly02]. The latter article succinctly states that almost every parameter $a \in [0,4]$ is either *regular* or *stochastic*. To be more precise, a parameter is called *regular* if Q_a has an attracting cycle. In this case the cycle is unique, and attracts almost all orbits in $[0,1]$. A parameter is called *stochastic* if Q_a has an absolutely continuous invariant measure. In this case, the measure is unique, and almost all orbits in $[0,1]$ are asymptotically equidistributed with respect to it.

For convenience, let us denote the set of regular parameters by $\mathcal{R}$, and the stochastic parameters by $\mathcal{S}$. The result by Lyubich then states that $|\mathcal{R}|+|\mathcal{S}| = 4$, where $|\cdot|$ denotes Lebesgue measure.

Today, it is well-known that $\mathcal{S}$ has positive measure, see e.g. [BC85], [BC91], [Ja81]. Remarkably, until very recently (see [LT06]), there has been no non-trivial estimates on the measure of $\mathcal{S}$. And, as the authors of [LT06] point out, the result[1] $|\mathcal{S} \cap I^*| > 0.97|I^*| > 10^{-5000}$ with $I^* = [2 - 10^{4990}, 2]$ is not a good estimate of $|\mathcal{S}|$. Seeing that $\mathcal{R}$ is an open (and dense [Sw92]) set, it trivially follows that it has positive measure. The aim of this work is to try to obtain a good *lower* bound on the measure of $\mathcal{R}$. In light of [Ly02], this automatically translates to a good *upper* bound on the measure of $\mathcal{S}$.

Theorem 1 (Main Theorem) *The set of regular parameters for the quadratic map satisfies the lower bound:* $|\mathcal{R} \cap [2, 4]| \geq 1.61394824439594656781$.

We believe that this lower bound is quite close to the true measure. According to non-rigorous numerical experiments ([Si08]) the measure of the regular set, beyond the first period doubling cascade (at $r^\star \approx 3.569945672$) is estimated to be $|\mathcal{R} \cap [r^\star, 4]| \approx 0.0455857$, i.e., $\mathcal{R}$ constitutes roughly 10.6% of the set $[r^\star, 4]$. Our bound captures more than 10.2% of these parameters, which means that our rigorous result is just slightly less than the non-rigorous estimate. Of course, the non-rigorous estimate may be a gross underestimation of the actual measure, but we find this quite unlikely.

The way we obtain our main result is by adaptively partitioning the parameter space $\mathbb{A} = [2, 4]$ into subintervals. For each such subinterval $\mathbb{A}_i$, we attempt to prove that Q_a has a unique, stable periodic orbit, which persists for all $a \in \mathbb{A}_i$. This can be achieved by employing various set-valued versions of fixed point theorems, implemented rigorously using interval analysis.

We also prove the existence of period doubling bifurcations, using a method presented in [WZ09]. Note that, although the set of parameters at which a period doubling occurs has measure zero, this step is not entirely superficial. It allows us to join the two parameter sets that correspond to stable periodic orbits before and after a period doubling. This produces larger connected parameter sets within each period doubling cascade, and thus adds measure to our final bound.

2 Three methods for verifying the existence of a stable orbit

Our algorithm for computing a lower bound for the measure of $\mathcal{R}$ uses the following three methods for verifying the existence of a stable orbit:

- the Brouwer theorem,
- the method of backward shooting,
- the modified interval Krawczyk operator.

[1] This results concerns the quadratic map $f_b(x) = x^2 - b$. Thus the parameter $b = 2$ corresponds to our parameter $a = 4$.

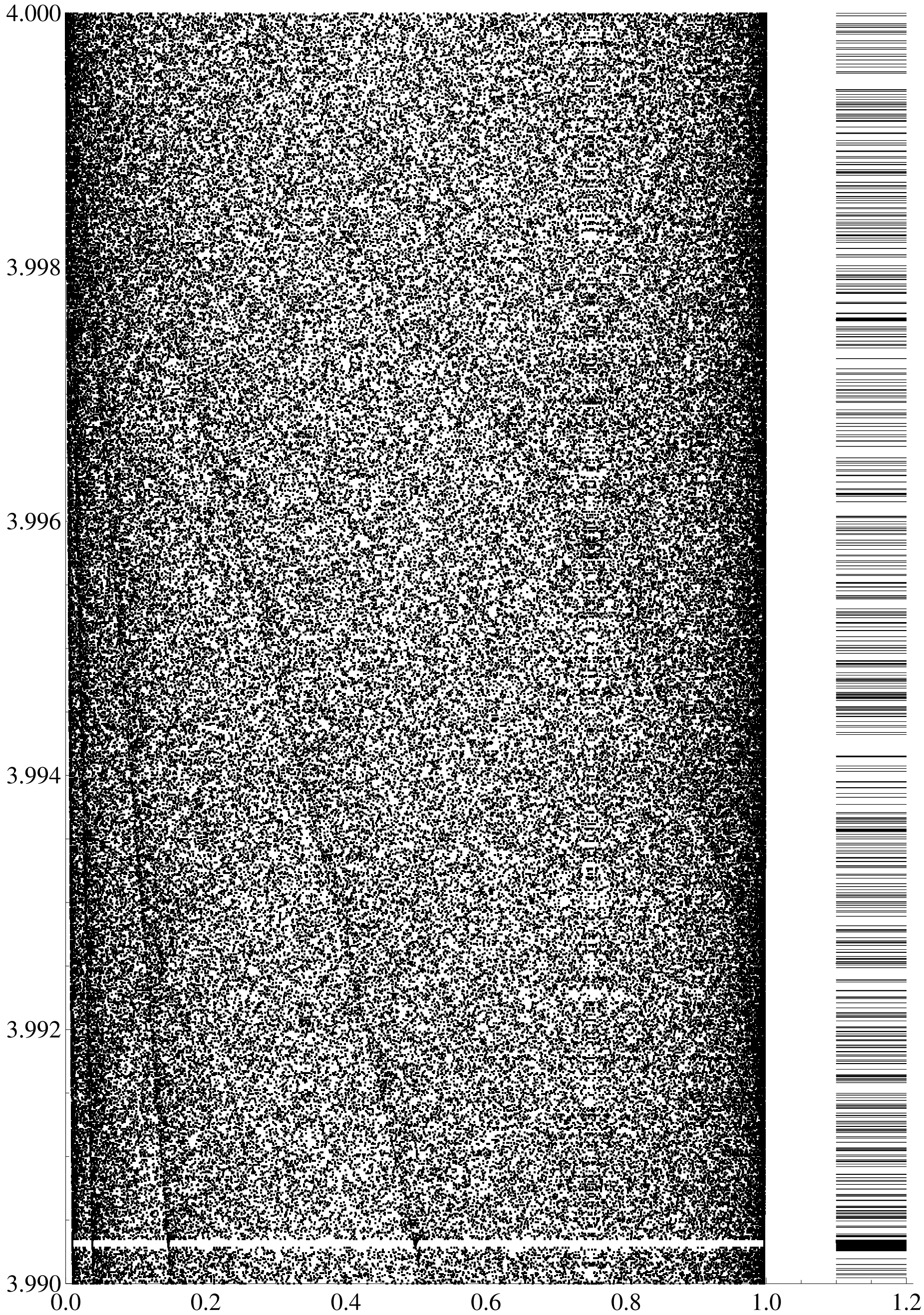

Figure 1: The bifurcation diagram for the quadratic map for parameters $a \in [3.99, 4]$. To the right of the main bifurcation diagram, verified stable windows have been marked as black rectangles.

The three methods are increasing in computational complexity, and therefore, when proving the existence of a stable orbit, we first use the Brouwer theorem. If this method fails, we apply the method of backward shooting. If we still have no success, we switch to the modified interval Krawczyk method, provided the assumptions of this method are satisfied.

2.1 The method based on the Brouwer theorem

This is the simplest method, and it relies upon the fact that our goal is to prove the existence of a stable periodic orbit. Let $\mathbb{A}$ be a closed interval of parameters for which we expect the existence of a stable periodic orbit for Q_a. Let x_1 be an approximate p-periodic point for the parameter $a = \operatorname{mid}(\mathbb{A})$ and let X_1 be a closed interval containing x_1 in its interior. Using interval arithmetic we compute the sequence X_i, $i = 2, \ldots, p$ such that for all $a \in \mathbb{A}$

$$Q_a(X_i) \subset X_{i+1}, \quad i = 1, \ldots, p-1$$

Since the orbit is expected to be attracting, it might happen that $X_p \subset X_1$. In that case the Brouwer theorem guarantees that for each $a \in \mathbb{A}$ there exists a fixed point $x_1^a \in X_1$ for the map Q_a^p. It remains for us to verify that $\{x_i^a\}_{i=1}^p$ is the p-periodic stable orbit for Q_a.

The verification that p is the principal period of x_1^a can be simply done by checking if the computed enclosure of the trajectory satisfies the condition

$$X_1 \cap X_i = \emptyset, \quad \text{for } i = 2, \ldots, p \text{ such that } i-1 \text{ divides } p \tag{2}$$

In order to verify the stability of the trajectory of x_1^a it is enough to check if

$$|Q'_{\mathbb{A}}(X_1) \cdot Q'_{\mathbb{A}}(X_2) \cdots Q'_{\mathbb{A}}(X_p)| < 1 \tag{3}$$

Summarizing, we had prove the following

Lemma 2 *Assume that Algorithm 1 is called with the arguments $\mathbb{A}$ and X_1. If the algorithm stops and returns true then for each $a \in \mathbb{A}$ the computed enclosure $(X_1, \ldots, X_p)$ contains the unique p-periodic stable orbit for Q_a.*

The above method is very fast, but has some disadvantages compared to the methods described in the following sections. First, given that we always examine an interval of parameters $\mathbb{A}$ rather than a single parameter, the condition $Q_{\mathbb{A}}(X_p) \subset X_1$ might fail.

Second, the initial interval X_1 cannot be too small since we intend to verify the existence of a stable orbit for an interval $\mathbb{A}$. As the "convergence" of X_1 to the periodic orbit is linear (like the contraction of the map), it is very weak for parameters close to bifurcation parameters. Therefore the computed enclosure $(X_1, \ldots, X_p)$ of the periodic orbit may be quite wide. This fact can result in that the stability criterion (3) is not satisfied.

The methods described in the next sections avoid such disadvantages. The computational complexity, however, is larger.

Algorithm 1: verify stability by means of the Brouwer theorem

Data: $\mathbb{A}$ - interval,
$X_1, \ldots, X_p$ - intervals

begin
  for $i \leftarrow 2$ **to** p **do**
    $X_i \leftarrow Q_{\mathbb{A}}(X_{i-1})$;
    if $p \mod i - 1 = 0$ **and** $X_i \cap X_1 \neq \emptyset$ **then**
      return false;
  if $Q_{\mathbb{A}}(X_p) \not\subset X_1$ **then**
    return false;
  $X_1 \leftarrow Q_{\mathbb{A}}(X_p)$;
  Interval product $\leftarrow 1$;
  for $i \leftarrow 1$ **to** p **do**
    product $\leftarrow Q'_{\mathbb{A}}(X_i) \times$ product;
  if not $|\text{product}| < 1$ **then**
    return false;
  return true;
end

2.2 The method of backward shooting

One of the most efficient methods for verifying the existence of isolated zeros for a map is the interval Newton method (see e.g. [AH83], [Kr86], [KN84]). Given a smooth function $F : \mathbb{R}^n \to \mathbb{R}^n$, an interval vector[2] X, and a point $\bar{x} \in X$ we define the interval Newton operator by

$$N(F, \bar{x}, X) = \bar{x} - DF^{-1}(X)F(\bar{x}). \tag{4}$$

Theorem 3 *Let X be an interval vector, $\bar{x} \in X$, and $F : \mathbb{R}^n \to \mathbb{R}^n$ be smooth. Assume that $DF(X)$ is invertible as an interval matrix. If the interval Newton operator satisfies*

$$N(F, \bar{x}, X) \subset X$$

then the map F has a unique zero x^* in the set X. Moreover, $x^* \in N(F, \bar{x}, X)$.

This theorem can be adopted to the special situation of proving the existence of periodic orbits for one-dimensional maps, even for very high periods. In this section we recall the method of backward shooting introduced in [Ga02].

The question of the existence of a periodic point for a map $f : \mathbb{R} \to \mathbb{R}$ of principal period p can be transformed to finding a zero of the function

$$F(x_1, \ldots, x_p) = (x_2 - f(x_1), \ldots, x_p - f(x_{p-1}), x_1 - f(x_p)), \tag{5}$$

with the additional assumption that the zero of F has pairwise different coefficients. The following theorem is proved in [Ga02]:

[2] In the sequel we will call a Cartesian product of closed intervals an *interval vector*.

Theorem 4 *Let $X = (X_1, \dots, X_p)$ be an interval vector, $\bar{x} = (\bar{x}_1, \dots, \bar{x}_p) \in X$, and let $f : \mathbb{R} \to \mathbb{R}$ be a smooth map. Define F as in (5). Let us assume that A_k, G_k, H_k, $k = 1, \dots, p$ are intervals such that*

$$
\begin{aligned}
0 \notin A_k, &\quad k = 1, \dots, p \\
f'(X_k) \subset A_k, &\quad k = 1, \dots, p \\
f(\bar{x}_k) - \bar{x}_{(k \mod p)+1} \in G_k & \qquad\qquad\qquad (6)\\
\left(1 - A_1^{-1} \cdots A_p^{-1}\right) \sum_{i=1}^{p} A_1^{-1} \cdots A_i^{-1} G_i \subset H_1 & \qquad\qquad\qquad (7)\\
A_k^{-1}\left(H_{(k \mod p)+1} + G_k\right) \subset H_k, &\quad k = 2, \dots, p \qquad (8)
\end{aligned}
$$

Then $DF(X)^{-1}F(\bar{x}) \subset H = (H_1, \dots, H_p)$, and $N(F, \bar{x}, X) \subset \bar{x} - H$.

The above theorem gives a precise algorithm for proving the existence of periodic points for a map $f : \mathbb{R} \to \mathbb{R}$. If $\bar{x} = (\bar{x}_1, \dots, \bar{x}_p)$ is a good candidate for a periodic orbit, we can choose X to be a small interval vector centered at $\bar{x}$. Then, G_k and H_k can be computed directly by means of the formulas (6–8), provided that none of the A_k contain zero. If $N(F, \bar{x}, X) \subset X$, then by theorem (3) F has a (unique) zero in the set $N(F, \bar{x}, X)$, which corresponds to a periodic point of period p. As a final step, we must also verify that p is the minimal period of the found periodic point, and that this orbit is stable. This can be done by verifying conditions (2–3) in the same way as in Algorithm 1.

Remark 5 *In our algorithm, which verifies the existence of stable periodic orbits for the map Q_a, we use Theorem 3 applied to the map F defined as in (5) with $f = Q_{\mathbb{A}}$, where $\mathbb{A}$ is an interval of parameters. The interval Newton operator is computed as described in Theorem 4.*

The method of backward shooting, although very efficient, cannot be used to prove the existence of a superstable periodic orbit, or even an orbit which is very close to a superstable orbit. In this type of situation, we use a special version of the interval Krawczyk operator.

2.3 The interval Krawczyk method for superstable orbits

A superstable orbit appears when the critical point of Q_a is a periodic point. Let $(x_1, x_2, \dots, x_p)$ be a periodic orbit, and assume that x_1 is the critical point. It is easy to see that, in this situation, we cannot apply the backward shooting method, since $Q_a'(x_1) = 0$. Note, however, that the derivative of $F(x_1, \dots, x_p) = (x_2 - Q_a(x_1), \dots, x_p - Q_a(x_{p-1}), x_1 - Q_a(x_p))$ has the following form:

$$
DF(x_1, \dots, x_p) = \begin{bmatrix}
-Q_a'(x_1) & 1 & 0 & \dots & 0 \\
0 & -Q_a'(x_2) & 1 & \dots & 0 \\
\vdots & \vdots & \ddots & \vdots & \vdots \\
0 & 0 & \cdots & -Q_a'(x_{p-1}) & 1 \\
1 & 0 & \cdots & 0 & -Q_a'(x_p)
\end{bmatrix}.
$$

Since we are assuming that x_1 is a critical point, we have $Q'_a(x_1) = 0$. This means that the solution of the linear equation $DF(x_1, \ldots, x_p) \cdot y = z$, where $y = (y_1, \ldots, y_p)$, $z = (z, \ldots, z_p)$ is given by

$$\begin{cases} y_2 &= z_1 \\ y_3 &= z_2 + Q'_a(x_2)y_2 \\ y_4 &= z_3 + Q'_a(x_3)y_3 \\ \ldots & \\ y_p &= z_{p-1} + Q'_a(x_{p-1})y_{p-1} \\ y_1 &= z_p + Q'_a(x_p)y_p \end{cases} \tag{9}$$

Despite this, we cannot use this approach for superstable orbits when solving the linear equation by means of the interval Newton operator. This is because the coefficient $Q'_a(X_1)$ is then not equal to zero - it is an interval *containing* zero. Of course, one might consider using Gaussian elimination for solving the linear system which appears in the interval Newton operator. In this special case, however, the computational complexity can be significantly reduced by using the interval Krawczyk operator instead.

The interval Krawczyk operator is defined by

$$K(F, \bar{x}, X, C) = \bar{x} - C \cdot F(\bar{x}) + (\mathrm{Id} - C \cdot DF(X))(X - \bar{x}) \tag{10}$$

Theorem 6 *Let C be an isomorphism, and let $\bar{x} \in X$, where X is an interval vector. If the interval Krawczyk operator* (10) *satisfies*

$$K(F, \bar{x}, X, C) \subset \operatorname{int} X$$

then the map F has a unique zero in $x^* \in X$. Moreover, $x^* \in K(F, \bar{x}, X, C)$.

Observe that the method only requires that C be an (arbitrary) isomorphism. For the method to work well, however, C should be chosen to be an approximate inverse of $DF(\bar{x})$. The main idea of our approach for proving the existence of superstable periodic orbits (and also nearly superstable ones) is to choose the matrix J as an approximation of $DF(\bar{x})$, and then force the coefficient $J_{11} = 0$. Given this, we choose C to be the inverse of J, which always exists. Furthermore, it can be computed relatively fast – the computational complexity is quadratic with respect to the period p, as we will see below.

Another advantage, in comparison to Gaussian elimination, is that this approach is more memory efficient. In fact, we need not store neither C nor $\mathrm{Id} - C \cdot DF(X)$, which significantly decreases memory usage, especially for large periods – see Algorithm 2. The only storage we need to cater for are the values of $C \cdot F(\bar{x})$ and $(\mathrm{Id} - C \cdot DF(X))(X - \bar{x})$. The value of $C \cdot F(\bar{x})$ can be computed by means of (9). What remains for us to show is the algorithm for the computation of $(\mathrm{Id} - C \cdot DF(X))(X - \bar{x})$.

Lemma 7 *Assume that Algorithm 2 is called with its arguments, and assume that $a_1 = 0$. Then the algorithm always stops and returns an interval vector r*

Algorithm 2: solve linear system

Data: $a_1, \dots, a_p$ - scalars,
$A_1, \dots, A_p$ - intervals,
$\bar{x} = (\bar{x}_1, \dots, \bar{x}_p)$ - a vector,
$X = (X_1, \dots, X_p)$ - an interval vector

begin
  $r = (r_1, \dots, r_p)$: an interval vector;
  $r \leftarrow 0$;
  for $i \leftarrow 1$ **to** p **do**
    Interval product $\leftarrow A_i - a_i$;
    $r_{(i \mod p)+1} \leftarrow \big(r_{(i \mod p)+1} + \text{product} \times (X_i - \bar{x}_i)\big)$;
    for $j \leftarrow i+1$ **to** p **do**
      product $\leftarrow$ product $\times\, a_j$;
      $r_{(j \mod p)+1} \leftarrow \big(r_{(j \mod p)+1} + \text{product} \times (X_j - \bar{x}_j)\big)$;
  return r;
end

which is an upper bound for the interval vector $(Id - C \cdot D)(X - \bar{x})$*, where*

$$D = \begin{bmatrix} -A_1 & 1 & 0 & \dots & 0 \\ 0 & -A_2 & 1 & \dots & 0 \\ \vdots & \vdots & \ddots & \vdots & \vdots \\ 0 & 0 & \cdots & -A_{p-1} & 1 \\ 1 & 0 & \cdots & 0 & -A_p \end{bmatrix}, C = \begin{bmatrix} 0 & 1 & 0 & \dots & 0 \\ 0 & -a_2 & 1 & \dots & 0 \\ \vdots & \vdots & \ddots & \vdots & \vdots \\ 0 & 0 & \cdots & -a_{p-1} & 1 \\ 1 & 0 & \cdots & 0 & -a_p \end{bmatrix}^{-1}$$

Proof: It is easy to see that the matrix $M := \text{Id} - C \cdot D$ has the form

$$\begin{bmatrix} a_p \dots a_2 A_1 & a_p \dots a_3(A_2 - a_2) & \dots & a_p(A_{p-1} - a_{p-1}) & A_p - a_p \\ A_1 & 0 & \dots & 0 & 0 \\ a_2 A_1 & A_2 - a_2 & \dots & 0 & 0 \\ \vdots & \vdots & \ddots & \vdots & \vdots \\ a_{p-2} \dots a_2 A_1 & a_{p-2} \dots a_3(A_2 - a_2) & \dots & 0 & 0 \\ a_{p-1} \dots a_2 A_1 & a_{p-1} \dots a_3(A_2 - a_2) & \dots & A_{p-1} - a_{p-1} & 0 \end{bmatrix} \tag{11}$$

The above form can be obtained by the application of (9) to the columns of D. Hence, the coefficients of the matrix M are given by

$$M_{(j \mod p)+1,i} = \begin{cases} 0 & \text{for } j = 1, \dots, i-1 \\ A_i - a_i & \text{for } j = i \\ a_j M_{j-1,i} & \text{for } j = i+1, \dots, p \end{cases} \tag{12}$$

Define $r = (\text{Id} - C \cdot DF(X))(X - \bar{x})$. Then

$$r = \sum_{i=1}^{p} M_{\cdot,i}(X_i - \bar{x}_i), \tag{13}$$

where $M_{\cdot,i}$ denotes the i-th column of the matrix M. The above sum corresponds to the external loop in the algorithm indexed also by i. In the internal loop of the algorithm (indexed by j), the variable 'product' contains precisely the coefficients of the i-th column of the matrix M, as given by the recursive formula (12).

Since all operations used in the algorithm are always well defined in interval arithmetic (extended to NaN cases), the algorithm always returns a valid upper bound for $(\mathrm{Id} - C \cdot D)(X - \bar{x})$. ∎

The above lemma gives us a tool for computing the interval Krawczyk operator for a periodic orbit which is (or is close to) superstable. To be more precise: the interval Krawczyk operator is used to prove the *existence* of such a periodic orbit. In addition to this, we need to check if this orbit has principal period p, and if it is stable. As in the method of backward shooting one needs to verify the conditions (2–3).

3 A method for verifying the existence of period doublings for 1D maps

The methods described in the earlier sections allow us to prove the existence of stable periodic orbits for parameter ranges well separated from bifurcations. Our aim, however, is to give as good as possible lower bound for the measure of parameters for which stable periodic orbit exists. Therefore, it is important to take into account neighborhoods of parameters for which period doublings occur.

A period doubling occurs when the derivative of a stable periodic orbit decreases through the value -1. When crossing -1, a new stable periodic orbit arises, with a derivative slightly less than 1. The existence of the period doubling can be deduced just from higher derivative information of the map at the bifurcation point. This does not, however, give us any information about the size of the set, or the parameter range, on which we have such dynamics.

In the paper [WZ09], a method for proving the existence of period doubling for higher dimensional maps is proposed. In this method, some computable inequalities for the derivatives allow one to deduce the dynamics of a map in an explicitly given neighborhood of the bifurcation point – both in the phase space and in the parameter space.

Here we recall the main definitions and theorems, adopted to the one-dimensional case. Given a map $f : X \to Y$, we let $\mathrm{dom}\,(f)$ denote the domain of f. For a map $F : X \to X$, we will denote its (restricted) set of fixed points by $\mathrm{Fix}\,(F, U) = \{x \in U \mid F(x) = x\}$.

Definition 1 *Let $f : \mathbb{R} \supset \mathrm{dom}\,(f) \to \mathbb{R}$ be C^1. Let $z_0 \in \mathrm{dom}\,(f)$. We say that z_0 is a* hyperbolic fixed point for f *iff $f(z_0) = z_0$ and $|f'(z_0)| \neq 1$.*

Definition 2 *A subset $I \subset \mathbb{Z}$ is called an* interval in $\mathbb{Z}$ *if there exists an closed interval $[a, b]$, where $a, b \in \mathbb{R} \cup \{\pm\infty\}$ such that $\mathbb{Z} \cap [a, b] = I$.*

Definition 3 *Consider a map $f : \mathbb{R} \supset \operatorname{dom}(f) \to \mathbb{R}$. Let $x \in \mathbb{R}$. Any sequence $\{x_k\}_{k \in I}$, where I is an interval in $\mathbb{Z}$ containing zero such that*

$$x_0 = x, \qquad f(x_i) = x_{i+1}, \qquad \textit{for } i, i+1 \in I$$

will be called an orbit through x. *If $I = \mathbb{Z}_- \cup \{0\}$, then we will say that $\{x_k\}_{k \in I}$ is a full backward orbit through x.*

Definition 4 *Consider a continuous map $f : \mathbb{R} \supset \operatorname{dom}(f) \to \mathbb{R}$.*
Let $Z \subset \mathbb{R}^n$, $x_0 \in Z$, $Z \subset \operatorname{dom}(f)$. We define

$$\begin{aligned}
W^s_Z(z_0, f) &= \{z \mid \forall_{n \geq 0} f^n(z) \in Z, \quad \lim_{n \to \infty} f^n(z) = z_0\} \\
W^u_Z(z_0, f) &= \{z \mid \exists \{x_n\} \subset Z \textit{ a full backward orbit through } z, \textit{ such that} \\
&\qquad \lim_{n \to -\infty} x_n = z_0\} \\
W^s(z_0, f) &= \{z \mid \lim_{n \to \infty} f^n(z) = z_0\} \\
W^u(z_0, f) &= \{z \mid \exists \{x_n\} \textit{ a full backward orbit through } z, \textit{ such that} \\
&\qquad \lim_{n \to -\infty} x_n = z_0\} \\
\mathit{Inv}^+(Z, f) &= \{z \mid \forall_{n \geq 0} f^n(z) \in Z\} \\
\mathit{Inv}^-(Z, f) &= \{z \mid \exists \{x_n\} \subset Z \textit{ a full backward orbit through } z\ \} \\
\mathit{Inv}(Z, f) &= \mathit{Inv}^+(Z, f) \cap \mathit{Inv}^-(Z, f)
\end{aligned}$$

If f is known from the context, then we will usually drop it and use $W^s(z_0)$, $W^s_Z(z_0)$ etc instead.

Definition 5 *[WZ09, Def. 4] Let $f_a : \mathbb{R} \to \mathbb{R}$, where a belongs to some interval. We say that f_a has a* period doubling bifurcation *at (a_0, x_0) iff there exists $Z = [a_1, a_2] \times X \subset \mathbb{R} \times \mathbb{R}$, such that the following conditions are satisfied:*

- $(a_0, x_0) \in \operatorname{int} Z$, $f_{a_0}(x_0) = x_0$
- *there exists a continuous function $x_{fp} : [a_1, a_2] \to \operatorname{int} X$, such that*

$$\mathit{Fix}(f_a, X) = \{x_{fp}(a)\}$$

- *there exist two continuous curves $x_i : [a_0, a_2] \to \operatorname{int} X$, $i = 1, 2$, such that for $a \in [a_0, a_2]$, the following holds:*

$$\begin{aligned}
x_1(a_0) &= x_2(a_0) = x_{fp}(a_0) \\
x_1(a) &\neq x_2(a), \quad a \neq a_0 \\
f_a(x_1(a)) &= x_2(a), \quad f_a(x_2(a)) = x_1(a) \\
\mathit{Fix}(f_a^2, X) &= \{x_1(a), x_2(a), x_{fp}(a)\}
\end{aligned}$$

- *the dynamics:*

for $a \le a_0$

$$Inv(X, f_a) = \{x_{fp}(a)\}$$

and $x_{fp}(a)$ *is an attracting fixed point for* f_a*.*

For $a > a_0$ *the maximal invariant set in* X $Inv(X, f_a)$ *is equal to*

$$\overline{W^u_X}(x_{fp}(a), f) \cap \left(\overline{W^s_X}(x_1(a), f_a^2) \cup \overline{W^s_X}(x_2(a), f_a^2)\right)$$

and it is an interval connecting the points $x_1(a)$*,* $x_2(a)$*.*

Note that in the above definition, we assume the existence of a stable periodic orbit for each parameter value $a \in [a_1, a_2]$. Even for a_0, which has the neutral eigenvalue -1, the point x_0 is assumed to be attracting.

The following theorem summarizes the numerical method for proving the existence of a period doubling bifurcation for one-dimensional maps.

Theorem 8 *[WZ09, Thm.4, Thm.9] Let* $Z = [a_1, a_2] \times [x_1, x_2]$ *and let* $f_a : \mathbb{R} \to \mathbb{R}$ *be a family of maps, such that* $[x_1, x_2] \subset \mathrm{dom}\,(f_a)$ *for* $a \in [a_1, a_2]$*.*

A1 *Assume there exists a* C^k*-function* ($k \ge 3$)*,* $x_{fp} : [a_1, a_2] \to (x_1, x_2)$ *such that for* $a \in [a_1, a_2]$

$$Fix(f_a, [x_1, x_2]) = \{x_{fp}(a)\}$$

A2 *Assume that* $G : Z \to \mathbb{R}$*, defined as*

$$G(a, x) = x - f_a^2(x), \quad \text{for } (a, x) \in Z,$$

is a C^k*-function* ($k \ge 3$)*, such that*

$$\begin{aligned} \frac{\partial^3 G}{\partial x^3}(Z) &\subset (0, \infty) \\ \frac{\partial^2 G}{\partial x \partial a}(Z) + \frac{\partial^2 G}{\partial x^2}(Z) x'_{fp}([a_1, a_2]) \cdot [0, 1] &\subset (-\infty, 0), \\ \frac{\partial G}{\partial x}(a_1, [x_1, x_2]) &\subset (0, \infty), \\ G(a_2, x_2) > 0, \qquad G(a_2, x_1) &< 0, \\ \frac{\partial G}{\partial x}(a_2, x_{fp}(a_2)) &< 0. \end{aligned}$$

A3 *Assume that* f_a *is injective on* $[x_1, x_2]$ *for each* $a \in [a_1, a_2]$*, and*

$$\begin{aligned} f'_{a_1}(x_{fp}(a_1)) &\in (-1, 1), \\ f'_{a_2}(x_{fp}(a_2)) &< -1, \\ \frac{\partial}{\partial a}\left(f'_a(x_{fp}(a)\right) &< 0, \ \text{for } a \in [a_1, a_2]. \end{aligned}$$

Then there exists a point $(a_0, x_0) \in Z$ such that f has a period doubling bifurcation at (a_0, x_0), with the neighborhood from the definition of the period doubling equal to Z.

Let us observe that all assumptions from the above theorem can be verified using rigorous numerics. The existence of the fixed point curve x_{fp} can be established by means of the interval Newton method. Given an enclosure for $x_{fp}(a)$, we can compute its derivative $x'_{fp}(a)$ by differentiating the equation

$$x_{fp}(a) - f_a(x_{fp}(a)) = 0.$$

The other inequalities are easily handled using interval arithmetic, as long as the set Z is a good candidate for the existence of the period doubling bifurcation.

4 The main algorithm

In this section, we will outline the main parts of the algorithm used to bound the measure of stable parameters.

4.1 Finding superstable windows

By a result of Douady and Hubbard ([DH07]), each stable window contains exactly one parameter yielding a superstable periodic orbit. Let $x(a_*)$ denote a new born fixed point for $Q^n_{a_*}$ which is an origin of a stable window. In each case $\frac{\partial}{\partial x}Q^n_{a_*}(x(a_*)) = 1$ and this derivative decreases to -1 along the fixed point curve $x(a)$ when the parameter a increases and results in the next period doubling bifurcation. Hence, for some parameter value a_0 we have $\frac{\partial}{\partial x}Q^n_{a_0}(x(a_0)) = 0$ and the orbit is superstable. This means that the critical point for the quadratic map is on the trajectory of $x(a_0)$.

The above considerations give us a method for detecting superstable orbits. It is enough to solve the equation

$$Q^n_a(\tfrac{1}{2}) = \tfrac{1}{2} \tag{14}$$

with respect to a. Since the above equation is polynomial of the degree 2^n it has finite number of solutions, and any method for detecting zeros of this polynomial may be used. In our application we do not need to estimate all solutions of (14) – in fact a lot of them are complex numbers or even when real, they are out of the range $\mathbb{A} = [2, 4]$. In our algorithm we use the Newton method; the details will be presented in the sequel.

Given a good approximation of a superstable periodic point, say $x(a_0)$, we can also estimate very roughly the size of the entire stable window. This can be done by using the Taylor approximation of the curve $\frac{\partial}{\partial x}Q^n_a(x(a))$, where $x(a)$ is a curve of period-n points. In the first approach, we can use the linear approximation. Put

$$s(a) = \frac{\partial}{\partial a}\left(\frac{\partial}{\partial x}Q^n_a(x(a))\right)$$

Clearly $s(a_0)$ gives us a linear approximation of how fast the stability of $x(a_0)$ changes. Hence, given that $\frac{\partial}{\partial x}Q^n_{a_0}(x(a_0)) \approx 0$, we can expect that the stable window is roughly

$$d(a_0) = [a_0 + 1/s(a_0), a_0 - 1/s(a_0)] \tag{15}$$

(note that $s(a_0) < 0$) or at least of this magnitude. It is possible to compute a higher order Taylor expansion of this curve (for example by means of automatic differentiation), and then solve for when it is equal to 1 and -1.

4.2 One iteration of the algorithm.

Assume we have some grid of the parameter domain

$$[2, 4] = \bigcup_{i \in \mathcal{I}} \mathbb{A}_i,$$

where the $\mathbb{A}_i$ are closed intervals (with non-empty interior) such that $\operatorname{int} \mathbb{A}_i \cap \operatorname{int} \mathbb{A}_j = \emptyset$ provided $i \neq j$. To each subinterval $\mathbb{A}_i$ from this grid we attribute one of the following four labels: `unchecked, verified, periodDoubling, small`. The first grid of the interval $\mathbb{A} = [2, 4]$ is created by subdividing the interval $\mathbb{A}$ into 100 equal parts; each subinterval in this primary partition is given the label `unchecked`.

Let $N > 1$ be the maximal period of the stable window we are searching for. This is a parameter of our algorithm, and it remains fixed throughout the computations. One iteration of our algorithm consists of the following steps:

1. Search for superstable orbits
2. Fill parameter gaps
3. Search for parameter domains that contain a stable window, but which are not necessary superstable
4. Fill parameter gaps
5. Scan for period doubling

Note that neither our method of searching for superstable orbits, nor the bisection (step 3 below) produces a uniform partition. Without this non-uniform process, the computational times would become enormous. Below we describe how each one of the above steps are realized.

Searching for superstable orbits. For each subinterval $\mathbb{A}_i$, we proceed as follows.

1.1 If the interval $\mathbb{A}_i$ has a width smaller than 10^{-17}, we label it `small`.

1.2 If the interval $\mathbb{A}_i$ is *not* labeled as `unchecked`, we leave it intact, and exit.

1.3 Set $a = \mathrm{mid}(\mathbb{A}_i)$. For each $n = 2, \ldots, N$ the point a is a seed for the standard Newton method which solves equation (14). In this way we obtain a sequence

$$\mathbb{B}_i = \left(\mathbb{B}_i^2, \mathbb{B}_i^3, \ldots, \mathbb{B}_i^N\right)$$

such that for $n = 2, \ldots, N$ either $\mathbb{B}_i^n = \{a_i^n\}$ if $a_i^n \in \mathbb{A}_i$ is a good candidate for the superstable orbit of the period n, or $\mathbb{B}_i^n = \emptyset$, otherwise.

1.4 If $\mathbb{B}_i^n = \emptyset$ for each $n = 2, \ldots, N$ then we leave interval $\mathbb{A}_i$ intact, and exit.

1.5 For each $\mathbb{B}_i^n = \{a_i^n\}$ we try to prove that such a superstable orbit of principal period n exists on the interval of parameters $\mathbb{A}_i^n = a_i^n + [-10^{-17}, 10^{-17}]$. If we are able to prove stability on the interval $\mathbb{A}_i^n$ then we set $\mathbb{B}_i^n = \{\mathbb{A}_i^n\}$, otherwise $\mathbb{B}_i^n = \emptyset$.

1.6 For each $\mathbb{B}_i^n = \{\mathbb{A}_i^n\}$ we proceed as follows. Using the estimation (15) we try to find two numbers $c_i^n, d_i^n \in \mathbb{A}_i$ such that c_i^n is as close as possible to the origin of the window $\mathbb{A}_i^n$ and d_i^n is as close as possible to the end of that window. Next, we try to prove the existence of a stable periodic orbit of period n on the intervals $\mathbb{C}_i^n = c_i^n + [-10^{-17}, 10^{-17}]$ and $\mathbb{D}_i^n = d_i^n + [-10^{-17}, 10^{-17}]$.

1.7 We replace $\mathbb{A}_i$ in the current partition by a set of intervals $\mathbb{A}_i^n$, $\mathbb{C}_i^n$, $\mathbb{D}_i^n$, on which we were able to verify stability and mark them as `verified`. We also insert the remaining parts of $\mathbb{A}_i$, and mark them as `unchecked`.

Filling parameter gaps The above method for finding superstable orbits produces a parameter set with many gaps. At this point of the algorithm, we scan our current partition, and try to locate and fill possible gaps in the computed stable windows. The key point is that we do not need to determine a period of a stable window. We assume that if two subintervals $\mathbb{A}_i$ and $\mathbb{A}_j$ with the same period are separated only by intervals marked as `unchecked`, these might form a gap.

Searching for parameter domains that contain a stable window, but which are not necessary superstable This step might seem superfluous at first, but it is very important for proving the existence of period doublings, as well as for extending the primary window of each detected period doubling cascade. Note that the primary window in a cascade has the largest measure in that cascade, so it is very important to extend this window as much as possible.

3.1 If the interval $\mathbb{A}_i$ has a width smaller than 10^{-17}, we label it `small`.

3.2 If the interval $\mathbb{A}_i$ is *not* labeled as `unchecked`, we leave it intact, and exit.

3.3 Subdivide the parameter $\mathbb{A}_i$ onto two equal parts; say $\mathbb{A}_{i,1}$ and $\mathbb{A}_{i,2}$. Both halves inherit the label of $\mathbb{A}_i$. For each of these parts, we perform the next steps.

3.4 Set $a = \mathrm{mid}(\mathbb{A}_{i,j})$, and try to determine (non-rigorously) whether the map Q_a admits a stable orbit or not (of any period from the range $2, \ldots, N$). If we are not able to find a good candidate for a stable orbit, we mark $\mathbb{A}_{i,j}$ as `unchecked`, and exit.

3.5 If we have a good candidate for stable orbit, we try to prove the existence of this orbit for the parameter domain $a + 10^{-17}[-1, 1]$. If this is not successful, we mark $\mathbb{A}_{i,j}$ as `unchecked` and exit.

3.6 Try to extend the existing stable orbit as much as possible to the left and to the right (this is what makes our partition non-uniform). Then insert to our partition the verified interval of stability, marked `verified`. If the verified domain of stability is not the entire interval $\mathbb{A}_{i,j}$, we also insert the remaining parts and mark them as `unchecked`.

Scanning for period doublings. In this step we traverse the current partition, and try to locate possible period doublings. For each candidate, we try to apply the method described in Section 3. If the method succeeds, we relabel the gap located between the two bounding stable windows as `periodDoubling`.

Collapsing data. In order to decrease the memory usage, we try to collapse windows which are connected, and on which we have the same verified period (it might happen that one window contains stability, the other period doubling).

5 Computational Results

In this final section, we present some quantitative results obtained from our computations.

In Table 1 we present information regarding the computed Lebesgue stability measure, the number of verified period doublings, and computational effort versus the subdivision level. From this table, it is apparent that proceeding with further subdivisions does not add much to the total stability measure, whereas the computational time increases significantly.

In order to obtain the stability measure reported in Theorem 1, we compute through 9 subdivision levels, with the restriction to the maximal period we are searching for as given in Table 1. We also compute through 18 subdivision levels with the restriction on the maximal period set to 33000, but with the older version of the C++ program, which did not contain the step of searching for superstable orbits. These latter computations took over one year of CPU time. We stress that this large computational effort is a consequence of us verifying the existence of orbits with relatively large periods (up to 33000). For such large periods, the corresponding stable windows do not contribute significantly to the total measure of the stability regions $\mathcal{R}$. Nevertheless, our aim is to maximize the lower bound of $|\mathcal{R}|$; not to be cost-effective. As a final step, we merge the data obtained from both computations. After merging the data, the number of verified period doublings numbered 95011.

level	N	measure	wall time (h:m:s)	per. doublings
1	256	1.60620127942955014935	2 : 05 : 05	14
2	256	1.61118596303518551971	3 : 05 : 08	78
3	256	1.61287812977207803823	1 : 43 : 51	335
4	256	1.61349027421762439933	2 : 39 : 44	1381
5	256	1.61372268390076635341	5 : 18 : 22	4019
6	256	1.61381346643292467144	8 : 47 : 48	9075
7	512	1.61389940246044893686	67 : 26 : 04	20128
8	512	1.61391413966146151119	95 : 46 : 06	41692
9	1024	1.61393868758488911574	2 months	89828

Table 1: Computational results in terms of the level of subdivision. Here, the reported wall time corresponds to the current subdivision level only, and is thus not the accumulated time. The listed values of the measure and period doublings, however, correspond to the accumulated amount from all previous levels.

In Table 2, we illustrate the fact that the parameter $a = 4$ is a (one-sided) Lebsgue density point of $\mathcal{S}$. As such, the relative measure of the regular parameters should tent to zero as the density point is approached.

δ	$\|\mathcal{R} \cap \mathbb{A}_\delta\|/\|\mathbb{A}_\delta\|$	$-\log_{10}(\|\mathcal{R} \cap \mathbb{A}_\delta\|/\|\mathbb{A}_\delta\|)$
10^{-1}	2.542×10^{-2}	1.595
10^{-2}	7.596×10^{-3}	2.119
10^{-3}	3.148×10^{-4}	3.502
10^{-4}	1.555×10^{-5}	4.808
10^{-5}	4.145×10^{-6}	5.382
10^{-6}	1.466×10^{-7}	6.834

Table 2: The relative measure of the stable set, localised to increasingly small sets $\mathbb{A}_\delta = [4 - \delta, 4]$.

In Figure 2, we illustrate an interesting phenomenom; when we plot $\log_2$ of the period versus $\log_{10}$ of the verified measure, all points appear to be confined within a wedge–shaped region. This was also observed in [ST91].

In Table 3 (see the Appendix) the verified lower bound for the total measure of stable windows with a given principal period is presented. Note that the measures do not sum to the total measure obtained in Theorem 1. This is because the sets on which the period doubling is verified is not taken into account in this table.

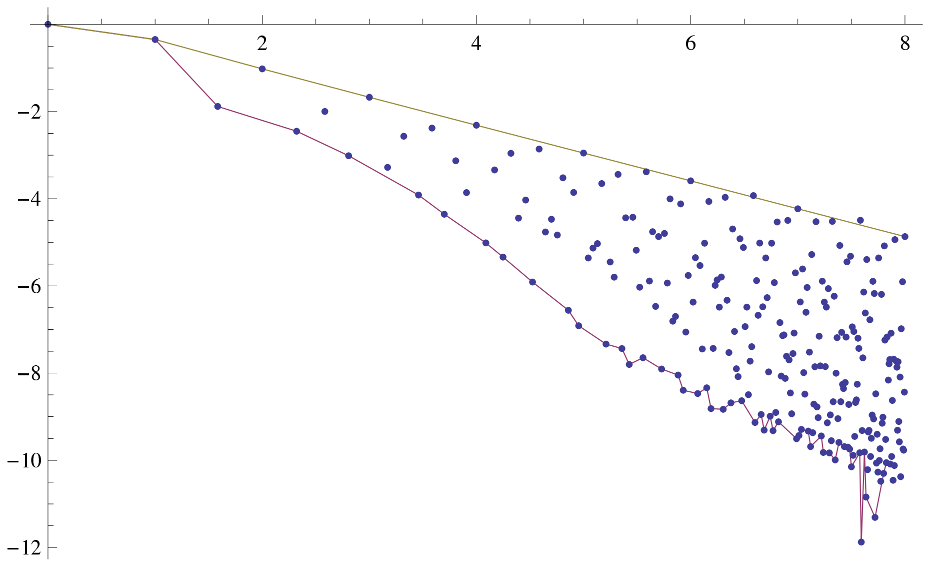

Figure 2: A plot of $\log_2$ of the period versus $\log_{10}$ of the verified measure. Note how the prime periods form the lower line, whereas periods of the form 2^k form the upper line.

5.1 Implementation notes

The program realizing the computer assisted proof of Theorem 1 has been written by the authors, and the C++ source code is available to download at [W]. The program has been successfully compiled and run on a 32 CPU computer (8 2.2 GHz Athlon Quad Processors) under the Fedora 10 operating system. During all computations, we use `long double` precision. The code, however, is independent of the number type, and supports e.g. GMP formats too.

The output of the program contains information about the intervals on which we are able to verify stability or period doubling, together with rigorous enclosures for such orbits. The file with this data is about 61GB, and is available from the authors on request.

Acknowledgements: The authors would like to thank Carles Simó for helpful comments and discussions on this topic.

References

[AH83] Alefeld, G. and Herzberger, J. *Introduction to Interval Computations.* Academic Press, New York, 1983.

[BC85] Benedicks, M. and Carleson, L. *On iterations of* $1 - ax^2$ *on* $(-1, 1)$. Ann. of Math., 122:2, 1–25, 1985.

[BC91] Benedicks, M. and Carleson, L. *The dynamics of the Hnon map.* Ann. of Math., 133:2, 73–169, 1991.

[CE80] Collet, P. and Eckmann, J.-P. *Iterated Maps on the Interval as Dynamical Systems.* Boston, MA: Birkhuser, 1980.

[DH07] Douady, A. and Hubbard, J. *Etude dynamique des polynômes complexes.* Documents mathématiques, Société Mathématique de France, 2007.

[Ep85] Epstein, H. *New Proofs of the Existence of the Feigenbaum Functions.* Inst. Hautes tudes Sco., Report No. IHES/P/85/55, 1985.

[Fe79] Feigenbaum, M. J. *The Universal Metric Properties of Nonlinear Transformations.* J. Stat. Phys. 21, 669–706, 1979.

[Ga02] Galias, Z. *Proving the existence of long periodic orbits in 1D maps using Newton method and backward shooting.* Topology and its Applications, Volume 124:1, 25–37, 2002.

[Ja81] Jakobson, M.V. *Absolutely continuous invariant measures for one-parameter families of one-dimensional maps.* Comm. Math. Phys., 81, 39–88, 1981.

[Kr86] Krawczyk, R. *A class of interval-Newton-operators.* Computing, Volume 37:2, 179–183. 1986.

[KN84] Krawczyk, R. and Neumaier, A. *An improved interval-Newton-operator.* Freiburger Intervall-Berichte 84/4, 1–26, 1984.

[La82] Lanford, O. E. III. *A Computer-Assisted Proof of the Feigenbaum Conjectures.* Bull. Amer. Math. Soc. 6, 427–434, 1982.

[LT06] Luzzatto, S. and Takahashi, H. *Computable starting conditions for the existence of nonuniform hyperbolicity in one-dimensional maps.* Nonlinearity 19, 1657-1695, 2006.

[Ly02] Lyubich, M. *Almost every real quadratic map is either regular or stochastic.* Ann. of Math., v. 156, 1–78, 2002.

[Ma76] May, R.M. *Simple mathematical models with very complicated dynamics.* Nature 261:459, 1976.

[Si08] Simó, C. Private communication, 2008.

[ST91] Simó, C. and Tatjer, J. C. *Windows of attraction of the logistic map.* In C. Mira et al.ed. *European Conference on Iteration Theory (ECIT 89), Batschuns (Austria)*, 335–342, World Scientific, Singapore, 1991.

[Sw92] Swiatek, G. *Hyperbolicity is Dense in the Real Quadratic Family.* Stony Brook IMS Preprint 1992/10.

[W] D. Wilczak, `http://www.ii.uj.edu.pl/~wilczak`, a reference for auxiliary materials.

[WZ09] Wilczak, D. and Zgliczyński, P. *Period doubling in the Rössler system - a computer assisted proof.* To appear in Found. Comp. Math., 2009. [DOI 10.1007/s10208-009-9040-x]

Appendix

p	N_w	verified measure
1	1	0.99999999999999999133
2	1	0.449489712730337562154
3	1	0.0130718827973174615657
4	2	0.0952673665554875199416
5	3	0.00352281749623573363014
6	5	0.0100535208500819814043
7	9	0.000970108705773774183598
8	16	0.0211991511740123133017
9	28	0.000524485461610248388312
10	51	0.00270572045435648776343
11	93	0.000121528614720657927514
12	170	0.00417709278913209851314
13	314	4.41799281499500023224e-05
14	583	0.000745338242653109531513
15	1081	0.00013866411367281154636
16	2001	0.00484464029931238248858
17	3674	9.73054144422376941781e-06
18	6571	0.000459303691807767637545
19	11206	4.62585472593029546629e-06
20	17602	0.00110323675556129436291
21	26270	3.58681690089041917135e-05
22	35999	9.30300639218476551479e-05
23	37228	1.25536973051955727532e-06
24	54621	0.00138359311074481676485
25	53658	1.72318055346306828191e-05
26	71167	3.38041935882169800737e-05
27	85069	1.4731351237678731031e-05
28	90545	0.000302802777599259741181
29	70699	2.92616749706254425378e-07
30	72811	0.000139073782564788119009
31	49998	1.32487884997936622433e-07
32	51460	0.00111489583255148854909
33	51338	4.37407428109876442179e-06
34	52969	7.41426465505293924574e-06
35	51517	9.33206508702726436622e-06
36	54577	0.000222757503877830161793
37	48407	4.88544719043620262466e-08
38	53694	3.54432509872947693053e-06
39	42923	1.58656653860079002727e-06
40	52635	0.000360875968039200316698
41	36336	3.77527918547174851094e-08
42	50684	3.65605909414580283051e-05
43	28864	1.69450330377539370996e-08
44	47615	3.75116589486691222322e-05
45	21957	6.61146604233418117014e-06
46	43808	9.44120952634311394469e-07
47	14255	2.30083172458005191796e-08
48	42503	0.000415087370009211385768
49	9915	1.29714218588755994532e-06
50	38085	1.75737844581981637188e-05
51	9566	3.41429440874627468383e-07
52	36585	1.35894747589091011847e-05
53	5303	1.26399147778229886674e-08
54	38727	1.59944966324214628284e-05

p	N_w	verified measure
55	3834	1.16952087014289031475e-06
56	34696	9.88223384075245878805e-05
57	7775	1.57651265319863273517e-07
58	33002	2.04086492206802250227e-07
59	2263	9.39608159702433332061e-09
60	40112	7.60159858456679275035e-05
61	1712	4.2499394036551313425e-09
62	32056	9.15700806604358152896e-08
63	8587	1.73677949005996735965e-06
64	33904	0.000256549465339254555846
65	1853	4.26198131763802154359e-07
66	39564	4.45155419376936853371e-06
67	980	3.5057975281485576069e-09
68	34003	2.93812095214789244235e-06
69	9099	3.72479415880911518544e-08
70	30358	9.57473156841894858238e-06
71	599	4.69818209791923735441e-09
72	42865	8.63683164619860350292e-05
73	481	2.02193056329964815365e-09
74	25233	3.78680588667985179585e-08
75	10964	1.03411117788700969433e-06
76	31668	1.38456132692103307813e-06
77	1242	3.26382623013713596416e-07
78	30007	1.60349387493246425818e-06
79	331	1.89875125409903755536e-09
80	33257	0.000107430044875180116457
81	9330	4.7157074870756224283e-07
82	15542	3.05558143936807830032e-08
83	193	2.75592126463414244242e-09
84	38462	2.01670921383297063745e-05
85	3884	9.05240564882080211984e-08
86	10550	1.35961065155908861213e-08
87	8993	8.67064942349123068954e-09
88	26053	1.2129835051315034089e-05
89	98	2.39681285821129186342e-09
90	24006	7.60450007215125386995e-06
91	1998	1.16842960114346347544e-07
92	22564	3.2889032366045962974e-07
93	8526	3.32452233689321807741e-09
94	5041	1.91490069276472468784e-08
95	5369	4.09062863484643129963e-08
96	34853	0.000117737286417092437002
97	44	9.6037879840533968423e-10
98	6033	1.32695184839161720025e-06
99	9140	2.12315322532059466698e-07
100	26510	9.65785966405342290175e-06
101	33	1.48979659533345076827e-09
102	14987	3.32312031203416125003e-07
103	35	6.26427760141642919756e-10
104	21894	4.37396446778320555082e-06
105	15452	5.39741123959215987616e-07
106	1846	1.081138791252794773e-08
107	27	1.35893234555831132759e-09
108	33467	9.58279471456168624455e-06
109	19	5.89864870923634265765e-10

p	N_w	verified measure
110	10150	1.19038627957698990578e-06
111	4657	1.33885744092905600855e-09
112	25245	2.93651594566893357069e-05
113	22	7.62790269967159040299e-10
114	14037	1.44886106519638915846e-07
115	6379	8.9113670026074592867e-09
116	17449	7.36887705993227726253e-08
117	6022	7.55974681727975689194e-08
118	855	7.6775308235476485974e-09
119	4457	2.4378422289758963637e-08
120	43913	3.18881550352232562284e-05
121	1712	2.01468847724553534739e-08
122	684	3.88504109156799504188e-09
123	1979	1.17893921296359505124e-09
124	16585	2.86872655920998587131e-08
125	6388	8.27675618213837699377e-08
126	21280	1.99476268637191131439e-06
127	10	3.11803653426159788076e-10
128	22271	5.90094534758855895212e-05
129	1334	3.98103039249420032064e-10
130	11056	4.29632068925552002003e-07
131	15	5.12374432161746828918e-10
132	31059	2.44424912292508060563e-06
133	5116	1.03566685637646732632e-08
134	359	3.30075103274068970549e-09
135	11331	2.49496996281278055063e-07
136	21508	9.22704891692530462799e-07
137	7	4.88723072645039224859e-10
138	12129	3.08445294360058103189e-08
139	6	2.2263665975900959193e-10
140	29225	5.27134620044726782961e-06
141	632	4.44651497262874006999e-10
142	205	1.9515967544271595191e-09
143	4612	1.40176287606510324713e-08
144	40197	2.98354731677204741691e-05
145	5540	1.72202841721390276231e-09
146	164	1.13737421173973340949e-09
147	5744	7.01726367217762880824e-08
148	9725	1.47993973707849502119e-08
149	7	4.7965822481434161606e-10
150	22985	1.28595427839779674617e-06
151	6	1.55892453460038105106e-10
152	19472	4.27804169227195135727e-07
153	5541	1.41867695212932742876e-08
154	11318	3.26390295524994419885e-07
155	4733	7.744848803080406352e-10
156	23718	8.70282784781739593427e-07
157	4	1.48039428155347096983e-10
158	95	1.23036237101303846941e-09
159	255	2.82154136209758488185e-10
160	30501	3.03247317811551793387e-05
161	5273	2.26044629563805499206e-09
162	16539	5.81770673163456084054e-07
163	6	1.01781208678222712116e-10
164	4320	1.00819781626970000898e-08
165	8982	6.4926658942861953383e-08
166	61	2.43698963764936438192e-09
167	3	3.3115959735714739498e-10
168	39995	8.48901984030646025725e-06

p	N_w	verified measure
169	2552	2.23272062990775843616e-09
170	11995	8.61908283987088824629e-08
171	5301	5.61112843623819135264e-09
172	3013	4.68261720869798947486e-09
173	4	2.05689922993385065908e-10
174	9899	6.12742601146035181792e-09
175	7178	6.69645084715262545183e-08
176	21688	3.57028187807518354591e-06
177	111	2.09676764449315267136e-10
178	28	1.91676241458743623625e-09
179	1	1.81419202577304261581e-10
180	37873	4.79193552861841530477e-06
181	2	7.09528416922844407111e-11
182	11798	1.1485544300165149989e-07
183	90	1.31884991859745892562e-10
184	14009	9.11574432392418809723e-08
185	1472	3.6963785938343152182e-10
186	8445	2.14654189540329498609e-09
187	4889	2.44808127545723119844e-09
188	1488	5.7186869608250728847e-09
189	8877	6.33191324262306204362e-08
190	10914	3.71763664193391907276e-08
191	1	1.49110541839206356407e-10
192	32702	3.2177302876180285951e-05
193	8	9.00781276826079224662e-11
194	21	4.82311795970552514845e-10
195	6482	2.25026412384397161981e-08
196	10147	7.25032295128625117742e-07
197	2	2.00523780739814139196e-10
198	19072	2.38974888486839093238e-07
199	6	9.19185515462633828676e-11
200	23926	4.04666939301232854442e-06
201	44	6.48903123075250665153e-11
202	17	4.4796317133152796508e-10
203	2893	5.39752981242383467197e-10
204	17214	1.68595043458560217564e-07
205	619	1.23161830126866655988e-10
206	16	3.21873659453117411111e-10
207	4162	1.12593208476292894193e-09
208	19960	1.2720479569726730884e-06
209	4250	8.93307148738808898258e-10
210	26945	6.72630792430614632416e-07
211	6	6.63180751633851706117e-11
212	514	3.39555334023800003962e-09
213	14	8.67556000996860809948e-11
214	11	3.95234908169561638402e-10
215	381	5.35231091218502097462e-11
216	34527	4.39114458286615251537e-06
217	2075	1.02007570142517711709e-10
218	12	1.84614170738867100496e-10
219	18	3.29184882477684404023e-11
220	17958	6.40910974284607595775e-07
221	4056	7.12826590072365706696e-10
222	2948	9.87033731874101261106e-10
223	1	5.00427043553797190611e-11
224	25452	8.26527393371417548606e-06
225	6878	5.74246923296193451103e-08
226	8	3.95313851748665956443e-10
227	1	8.85771068038360143149e-11

p	N_w	verified measure
228	14414	6.71485239852904342017e-08
229	3	4.22294577778759006037e-14
230	8715	7.01471073870536809824e-09
231	5572	1.64611388341843328798e-08
232	9784	2.06922104112675087073e-08
233	2	8.1889808085586213l6e-11
234	13890	8.2372610413867716761e-08
235	196	1.22304312510923551827e-10
236	283	2.37998886375677398686e-09
237	12	4.01446688391704498144e-11
238	9773	2.11521022056189444971e-08
239	1	7.58494384921898356922e-11
240	47139	1.15839131623184533187e-05
241	2	3.64872628638712726001e-13
242	5664	1.89574562638617633015e-08
243	3024	1.36608150898102909121e-08
244	186	5.6582058678179836253e-10
245	1069	1.82342126109607399753e-08
246	1300	7.8424157987956599758e-10
247	3030	2.65798257752594691006e-10
248	8045	8.24204953744044066521e-09
249	2	4.22043962278184636716e-11
250	8005	1.04117474487288794172e-07
251	2	9.15279304170707463939e-11
252	30848	1.25053648183069687772e-06
253	2554	1.82116620612085555742e-10
254	7	1.92401124980007276477e-10
255	4431	3.71214327332669569159e-09
256	15768	1.35557317334816969379e-05
258	857	2.8773955679066431923e-10
259	461	3.69586024111245858847e-11
260	16402	2.25462528252859048528e-07
261	1821	1.93364146092514510578e-10
262	4	1.98707860062097285692e-10
263	1	2.87478591279310968787e-13
264	26670	1.01403571368540064424e-06
265	61	6.65218461912142622339e-11
266	8115	7.89302969880258109558e-09
267	9	3.38333571228699447886e-11
268	100	8.73613650170801392392e-10
269	1	7.64205300603226778122e-12
270	20647	3.28607137428833795401e-07
271	1	2.77743186522655394199e-11
272	15205	2.57170787834430647489e-07
273	3630	5.47343850755208083392e-09
274	4	1.80316350826409399488e-10
275	2162	7.95625608083182223051e-09
276	10154	1.36178319586500312655e-08
278	4	1.14461913688565508629e-10
279	1065	6.16223929522652369428e-11
280	26310	2.20120257767128686688e-06
282	427	5.42756389094664615236e-10
284	43	1.15193265061257210657e-09
285	3581	1.3467319453629861 27e-09
286	9544	1.16034874009587896104e-08
287	162	3.00718781473530150095e-11
288	37360	9.56688468063378663619e-06
289	778	3.35680834257640059448e-11
290	5004	1.25910311365474980594e-09

p	N_w	verified measure
291	3	3.28789100979831605542e-12
292	34	2.48037972756451341461e-10
294	8555	8.72918724690793790266e-08
295	22	3.28098236513502117262e-11
296	2675	3.04630167445585353647e-09
297	3028	6.90054067142495397569e-09
298	3	1.77444756587971652628e-10
299	1203	3.26468379240052453127e-11
300	25657	8.60520799162789798431e-07
301	107	7.98897059617331706249e-12
302	1	1.05277613883514309379e-12
303	2	2.13528411532187822885e-11
304	12325	1.13558001946451395114e-07
305	20	1.17904477413971475741e-11
306	9108	1.24334928052090287753e-08
308	14963	1.69071440280074355988e-07
309	5	1.29976884290228245078e-11
310	3466	3.13585505435851064071e-10
312	20269	3.52741314715247084033e-07
314	1	1.34669061926245836602e-11
315	5468	2.92710065927324208923e-08
316	23	2.66370204539401189692e-10
318	152	2.72538734419000561182e-10
319	488	2.25722775974018796674e-11
320	24319	8.24290176316207386098e-06
322	5453	1.56525023129426565927e-09
323	856	1.62678670447696793744e-11
324	17339	3.91494915783678967824e-07
325	1377	2.43611868460009983739e-09
326	2	1.02464694715087567545e-13
327	1	6.57320638891567554651e-12
328	1083	2.75245310397964626503e-09
329	55	2.05206027951293501488e-11
330	13569	7.73379561030095030727e-08
332	19	3.00797065640873162451e-10
333	181	1.62291148401993989836e-11
334	3	1.24433050452052440527e-10
335	3	8.42931562224091823765e-12
336	35084	3.07296043592221283791e-06
338	3720	1.49485684486187764275e-09
339	1	1.89858207280679813778e-11
340	11114	3.7674688509094916844e-08
341	213	4.20183722885103527744e-12
342	7272	4.30791115887257936024e-09
343	179	1.58285188471898874418e-09
344	727	6.25700079855823210195e-10
345	1986	2.44466277299695833314e-10
346	1	1.04354091123512460193e-10
348	5374	3.01459598017923824376e-09
350	6967	8.38579626259716714998e-08
351	2168	2.01434204928109539257e-09
352	17305	9.8525265833544761751e-07
354	73	1.41771797209852556954e-10
355	4	2.03310424051750260332e-11
356	7	5.20716608937502045684e-10
357	1986	7.11454540896702680719e-10
358	2	6.39165695197341232614e-12
360	39653	2.27164097681164557641e-06
361	189	1.31565505018249595537e-12

p	N_w	verified measure
362	2	3.57109459191151668023e-12
363	1058	7.50220272190127435152e-10
364	12402	5.39704113264576762488e-08
365	3	6.46248245889102790329e-12
366	44	6.30018912473745418268e-11
368	7639	2.17337372400254469351e-08
369	79	1.35921094258223407181e-11
370	696	1.01923816608895378977e-10
371	15	1.20559738407688410433e-11
372	3710	8.59887850377175078087e-10
374	5548	1.37237300039741438873e-09
375	2133	6.13670979245257985912e-09
376	341	1.03754141996675874893e-09
377	126	3.69796315964621147288e-12
378	12656	8.23235203118756475593e-08
380	8644	1.36420115978436867765e-08
381	1	5.78295224207270308625e-13
384	24301	8.54806273583403816718e-06
385	1452	3.80935803994536525963e-09
387	36	1.01368408025187539678e-11
388	8	1.27831768174241355851e-10
390	10186	2.36231673838346173389e-08
391	151	8.98662437867625563115e-13
392	8863	2.93758243392503934355e-07
393	1	9.68506958659576255855e-14
395	1	1.06436365797379917097e-12
396	17783	1.37705456141950718929e-07
399	1511	2.36415917224952476516e-10
400	17274	1.45882010717831960001e-06
402	17	2.79695370596771963889e-11
403	54	1.28929419224155239476e-13
404	5	1.30888859863412254647e-10
405	2949	7.9489685231217549477e-09
406	1653	2.47670214415310341316e-10
407	36	1.49791594059034416375e-12
408	12078	5.82089477283061207391e-08
410	254	7.62303805149078250736e-11
412	6	4.54929832954115154209e-11
413	7	6.13906343295556045092e-12
414	4262	7.8518312121231281786e-10
416	14202	3.42896459139306955533e-07
418	3779	3.91484720292309407164e-10
420	25512	4.40697868522941377245e-07
423	25	9.72044189931353663781e-12
424	125	1.17792197328568659653e-09
425	777	3.18581583206092866511e-10
426	13	1.10871804358952941172e-10
427	5	1.44398121931788026018e-12
428	7	7.92441947564809234805e-11
429	1679	3.92744689201030006132e-10
430	185	4.49575108044109050809e-11
432	27587	1.7156002897675531188e-06
434	873	7.70161517026080044701e-11
435	525	2.53035528727935110638e-11
436	3	3.34855932045130533226e-11
437	57	1.13795257938864580183e-13
438	13	2.08447898698838063325e-11
440	15202	2.51972708386000512903e-07
441	1634	3.34070945668014929186e-09

p	N_w	verified measure
442	3463	2.74188517593657032911e-10
444	731	2.79526294038462408409e-10
448	17621	2.22956795963968196217e-06
450	10607	7.57204546679175055646e-08
451	8	1.48102016761519905685e-14
452	6	7.67666245241743760985e-11
455	1431	1.09358174729332069397e-09
456	8882	2.14739260472832788063e-08
458	1	3.59269471811307639086e-12
459	1157	2.13471115567340219421e-10
460	5063	2.60526625880247442169e-09
462	7375	1.71827184789613562899e-08
464	3299	4.81598111520473159963e-09
465	250	1.55688645569335148977e-11
468	12999	4.17045969132532473589e-08
469	4	1.52211403203761364011e-12
470	95	5.82505365557400844878e-11
472	60	1.81495567489961540097e-10
473	7	2.0804712119737445164e-13
474	8	1.41754409859612406919e-11
475	656	1.01225277292227300308e-10
476	6957	6.95506201372694810026e-09
477	5	4.10505375351977175313e-12
480	35258	3.81751390036012654139e-06
481	6	6.25016531585753654099e-14
483	747	4.27292923266264779159e-11
484	4644	7.01006428079076204796e-09
486	3947	1.66409927274645264017e-08
488	35	1.56188864576176089649e-10
490	2385	2.13134221395926137799e-08
492	270	1.37161591112766600986e-10
493	12	2.92234986210004876739e-13
494	1938	6.64124952948208502335e-11
495	2570	2.57108297564527521484e-09
496	2103	1.20387539672382748446e-09
497	2	4.21214278734094449419e-13
498	6	2.58419993303532491424e-11
500	4994	6.93831075523031193253e-08
501	1	7.29035972216185435002e-13
502	1	2.55261686354230077356e-11
504	25618	5.76997125744998715091e-07
506	1295	5.69910882809027130591e-11
507	605	3.9476151080658494763e-11
510	5237	2.89461418246164670087e-09
512	8535	3.10252627675313211175e-06
513	740	6.60282961119362798996e-11
516	137	6.39748306413556733219e-11
517	1	3.45381275662637321489e-14
518	137	2.15820358546309210013e-11
520	10622	8.09910322694448042702e-08
522	772	1.31615968124165760855e-10
524	2	5.00820494016979145258e-11
525	1832	3.68628364617006043513e-09
527	4	1.73259843971873550572e-14
528	15460	3.51311202236503569707e-07
529	1	1.03411203211667412916e-15
530	12	4.31274237242679214788e-11
531	1	1.01114277541169972352e-12
532	4245	2.16707579745595291243e-09

p	N_w	verified measure
534	4	1.2398985267322859 5492e-11
536	13	9.70846107499478971903e-11
539	521	4.18010325789128223128e-10
540	17481	2.2595014129893689625e-07
544	6817	5.99732031206917648447e-08
546	4516	4.97210680310347652444e-09
548	1	4.32844081757477461281e-12
549	2	5.01807796704500930218e-14
550	2453	8.20141227955879792422e-09
551	2	1.94933045399858784208e-14
552	3902	3.77969791749699357553e-09
555	29	1.199099630352917778e-12
556	1	2.07384884005207270619e-11
558	339	1.57733427014195015659e-11
559	1	2.18033056886834941679e-15
560	15519	7.78378122461400104304e-07
561	518	2.63372203820194661361e-11
564	70	5.73818048198865282572e-11
567	1125	1.95572463822582531812e-09
568	6	7.36877859078277630545e-11
570	3109	9.54028078325314110586e-10
572	5463	3.36500545071623247129e-09
574	29	1.59520187857642437024e-11
575	220	1.24981166908788576819e-11
576	22115	2.88741770726528949875e-06
578	368	6.47742211430657466309e-12
580	976	3.80496402831512203768e-10
582	3	5.17805546704219743503e-12
584	3	2.79572842740855032062e-11
585	1524	6.52993548339378393486e-10
588	6379	5.5688767369201086499e-08
590	3	1.2258972266129819495e-11
592	299	3.22638371314659666567e-10
594	3767	6.9994637444999868725e-09
595	606	1.03685408566270287345e-10
596	1	1.61110708107869982086e-13
598	361	1.05182440448409186828e-11
600	15095	4.18218123712310943518e-07
602	19	2.99426022171145334028e-12
604	1	1.13650885577576410412e-12
605	480	1.32555783190213549716e-10
608	4374	2.04285658239860418162e-08
609	76	4.23626910460439543016e-12
610	1	1.72474881598994045362e-14
611	1	2.46354586036501288504e-14
612	5061	4.13196899915965754069e-09
615	10	2.2658177417644864704e-13
616	8532	5.80411969985494130553e-08
618	2	2.97640406245192057355e-12
620	434	1.16514998387343138297e-10
621	195	7.49198880017898360961e-12
624	9613	1.11065251645137488823e-07
625	136	3.33101014436329445623e-10
627	278	4.88968761314101385551e-12
628	1	1.09057467917450523487e-12
629	1	1.62456853525227984392e-15
630	7956	3.56993611597047205697e-08
632	4	2.85736783626339141406e-11
636	18	5.01058127280740173148e-11

p	N_w	verified measure
637	334	8.40906476395897328757e-11
638	92	7.85749221764164840209e-12
640	11277	2.16519099872328375789e-06
644	1354	3.31289821964286801403e-10
645	3	4.50941367580171004192e-15
646	266	1.93933974781956841582e-12
648	9557	1.89861219263703917548e-07
650	1445	1.93038923669737461086e-09
651	28	5.51060932996172425646e-14
652	1	1.19616989924242744792e-13
654	1	6.59943020370201693936e-14
656	95	3.58436419867907973824e-10
658	9	9.20311461587164370002e-12
660	8720	4.20910504174334260119e-08
663	208	2.14897175575268217784e-12
664	3	4.29011732822753844019e-11
665	317	2.19077343072138219782e-11
666	51	5.08874973409456643481e-12
670	4	2.81208650115827296645e-12
671	1	5.96744875736021640478e-15
672	16585	9.90770461162075732897e-07
675	949	1.50169521696136287758e-09
676	1380	2.60235733136326974346e-10
678	2	5.32432518213221683823e-12
680	3589	8.55185064213212497997e-09
682	34	4.11202105352059810173e-13
684	2877	1.17970457469591949451e-09
686	507	1.72283972027856280285e-09
688	41	8.15190963777273625013e-11
690	911	1.14456457332712258079e-10
693	810	4.67717291546126956447e-10
696	581	6.4654358754821783517e-10
697	1	4.58465730657220404964e-15
700	3679	5.10405214651336869291e-08
702	2041	1.27188469868991238521e-09
704	6733	2.39798847709304929765e-07
705	6	2.92462516877922684699e-12
708	4	2.14708199136603994361e-12
710	2	2.78729817004830238147e-12
712	2	3.44888679247590257404e-11
714	1431	3.61813527922916211566e-10
715	457	3.62098382961778542111e-11
716	1	1.8762536663219364641e-11
718	1	1.15963705651922488471e-11
720	19213	8.64293335422518238 52e-07
722	59	3.1730347516134571606e-13
725	19	6.12616294498602442786e-13
726	924	3.34178100989956927691e-10
728	4729	1.26551819540181298418e-08
729	138	1.95599015716946267318e-10
730	2	4.18040168453925886638e-14
732	2	2.14005679496920286908e-13
735	518	9.76086386847083153917e-10
736	1434	3.44510321767695082418e-09
738	14	5.30566693010547929532e-12
740	57	2.81590068103299007163e-11
741	89	5.72940566517798899326e-13
742	3	4.77231904168207154981e-12
744	251	1.25631554421731794768e-10

p	N_w	verified measure
748	1408	1.50992142617170643781e-10
750	1344	7.56329652943157904055e-09
752	27	2.86284443417120226805e-10
754	20	1.62976403206283038116e-13
756	6432	4.79394160867851332197e-08
759	31	3.95866282462686847055e-13
760	1902	1.89107960367473904029e-09
765	343	3.31896912297152679727e-11
768	8604	2.18189426485549710366e-06
770	2004	2.75209809455501108744e-09
774	8	1.16522633555882215717e-12
775	6	9.12551284537599372015e-15
777	5	2.59859408296980731734e-13
780	4462	7.28152923026859077993e-09
782	31	2.15576688444851782833e-13
783	13	4.58466381178523896267e-13
784	3628	9.21655887939094170536e-08
792	6934	3.99928623729013665855e-08
793	1	2.05955044685346422284e-15
798	759	8.80575736026539823698e-11
800	5548	4.57099504875841528007e-07
804	4	7.40543694074946579065e-12
805	65	1.54558592486975232561e-12
806	4	1.93443351614863701116e-15
808	1	2.31145202804483584913e-11
810	2531	7.82668530636618231533e-09
812	114	3.9553866909222690218e-11
814	3	1.46636825945622994993e-13
816	2701	8.72972972642410693922e-09
819	373	6.59180286310262486538e-11
820	15	1.82129912280198924535e-11
824	1	2.50777480378938655292e-13
825	404	2.8227400299986327159e-10
826	1	8.99280649946376797743e-15
828	670	1.22388641322218605367e-10
830	1	6.37055512509032695334e-15
832	3600	6.89918706682675353381e-08
833	58	3.21869354086290471173e-12
836	635	3.62297210461381968827e-11
837	1	1.38387565296049785957e-15
840	9844	1.81910378552196938529e-07
845	65	1.0787484187174678496e-12
846	4	5.86597177082426313177e-13
847	95	7.2785443037265418198e-12
848	9	2.38588763112543289502e-10
850	409	1.03452779762897018045e-10
854	2	3.50107963453805126619e-13
855	184	6.33060032347032564104e-12
858	918	9.70563900516002719954e-11
860	7	3.59931008608871394472e-12
861	1	4.73371342124551119923e-14
864	9039	5.56894825449062019773e-07
867	10	7.55010203662420664728e-14
868	49	3.4550149199952251422e-12
870	101	1.30182648515331234051e-11
874	8	6.76357841261632231067e-14
875	90	2.9289056141350300333e-10
880	4583	5.88084942915265834751e-08
882	1350	3.01455380601577116462e-09

p	N_w	verified measure
884	409	1.19631114910145885943e-11
888	31	5.75977980588060489708e-12
891	205	4.88868116994833901146e-11
896	5012	5.48941543476602969442e-07
897	8	3.74479093567803289488e-14
900	4438	4.07473651951005544358e-08
902	3	2.52011952972530650641e-14
903	1	2.80981835021343329117e-15
904	2	1.64998425079138089089e-11
906	1	1.52516888007880879741e-14
910	776	3.02234676305065952384e-10
912	1428	2.64289139141268836219e-09
913	1	6.46264725762124569997e-14
915	1	1.58987406573274370203e-15
918	531	5.47849354857327108803e-11
920	481	2.5668242162844856491e-10
924	2656	4.36216550706546024596e-09
925	1	2.85192876259277028339e-14
928	222	5.91796759383603210303e-10
930	19	9.11678068107879546744e-13
931	25	4.63697873501200952262e-13
935	74	1.1840131739632164809e-12
936	3392	7.54518250200945927997e-09
938	1	2.00197931149448393739e-14
940	5	2.36675132617159000858e-12
944	3	3.19315060504088421567e-12
945	461	5.23403440163758282289e-10
950	201	2.38799997571287336839e-11
952	1116	6.44693606876092784042e-10
957	3	5.35474442564520813903e-14
960	10269	1.09647653844121249767e-06
962	3	2.20977749987305571722e-14
966	164	6.19565076326322738964e-12
968	975	8.25539695848212518037e-10
969	3	1.10918219053957045617e-14
972	1315	6.16193178188013945817e-09
975	158	2.37665922098867499201e-11
976	2	6.35772901338982343589e-13
980	1249	8.92045035776924122306e-09
984	6	1.45336735268147831945e-11
986	4	2.06468956515104551386e-14
987	1	3.02997644335833982154e-14
988	187	2.42684951995419950777e-12
990	1631	1.02758240783616672243e-09
992	109	1.71481747421667329867e-10
996	2	3.1094838075923503 24e-12
999	2	2.92064549628490155442e-14
1000	1111	2.92516899702121441207e-08
1001	63	1.10894344922118914809e-12
1008	7140	1.75993060460731196026e-07
1012	96	4.88267998081937104615e-12
1014	200	4.8241792505177016892e-12
1015	6	2.20514578819219764227e-13
1020	1025	3.52777066239817749249e-10
1024	2052	6.91056137385685081975e-07
1040	16	7.44776625354742760621e-11
1050	7	6.47966142547362622395e-11
1056	76	7.7612096313541684145e-09
1072	1	7.05499872931392157938e-12

p	N_w	verified measure
1080	138	1.26050035227295853524e-08
1088	5	4.27856838283377505228e-10
1092	1	2.01661604082303824725e-17
1100	5	4.45526298145648702587e-12
1104	1	2.01661604082303824725e-17
1120	156	1.26051267759818078074e-07
1125	1	2.01661604082303824725e-17
1134	1	5.26686875536308551915e-12
1140	1	2.01661604082303824725e-17
1144	1	2.01661604082303824725e-17
1152	255	6.10567644449304045007e-07
1170	1	2.01661604082303824725e-17
1176	24	5.56366844088607148677e-10
1184	1	2.01661604082303824725e-17
1188	2	4.03323208164607649451e-17
1200	157	5.58073092254366548426e-08
1215	1	2.01661604082303824725e-17
1216	3	1.59302432356511758371e-12
1224	4	8.06646416329215298902e-17
1232	24	4.69212817471448273565e-11
1248	25	2.34445507712316425497e-10
1260	22	5.99486903261198245119e-11
1280	153	4.29530000367519398941e-07
1296	88	9.42396631803225914847e-09
1300	1	2.01661604082303824725e-17
1320	18	2.09381784913725832453e-11
1344	181	1.70660756297841623153e-07
1350	1	1.64668621620289723495e-11
1352	1	2.01661604082303824725e-17
1360	2	4.03323208164607649451e-17
1368	2	4.03323208164607649451e-17
1372	2	4.03323208164607649451e-17
1386	1	2.01661604082303824725e-17
1392	1	3.93118697317174081718e-14
1400	25	1.32888534074351860603e-09
1408	41	1.35467981270554621576e-08
1428	1	2.01661604082303824725e-17
1440	292	1.19849110882547932322e-07
1456	3	6.04984812246911474176e-17
1458	2	4.03323208164607649451e-17
1500	11	7.61010807322215487858e-11
1512	19	1.0492414099019797824e-10
1520	2	4.03323208164607649451e-17
1536	170	4.36508358502354920638e-07
1540	4	8.06646416329215298902e-17
1560	4	8.06646416329215298902e-17
1568	29	4.11252392557015511443e-09
1584	13	7.48487556656574071212e-12
1600	93	8.37857453239547467216e-08
1620	12	2.47292923985509283114e-11
1632	4	1.75302552422179624969e-11
1664	10	3.41086777528795681569e-10
1680	121	5.40150254342217084336e-09
1728	208	9.33806746942957704993e-08
1744	1	2.3505438047355386999e-12
1760	21	7.20544088804453419783e-11
1764	1	2.01661604082303824725e-17
1792	65	9.26499040202876517069e-08
1800	50	7.92415121584136294963e-10

p	N_w	verified measure
1824	4	8.06646416329215298902e-17
1848	4	8.06646416329215298902e-17
1872	6	1.20996962449382294835e-16
1904	1	2.01661604082303824725e-17
1920	262	2.163420860449693367e-07
1944	9	1.81495443674073442253e-16
1960	4	1.40516183758099266754e-11
1980	1	2.01661604082303824725e-17
2000	15	1.29177164234425823075e-09
2016	125	4.52573798142424932323e-09
2040	3	6.04984812246911474176e-17
2048	43	1.35853521534765042666e-07
2080	5	1.00830802041151912363e-16
2100	8	1.6132928326584305978e-16
2112	22	2.01244349526744081835e-10
2156	1	2.01661604082303824725e-17
2160	92	1.56601677936060723617e-09
2176	1	2.01661604082303824725e-17
2184	1	2.01661604082303824725e-17
2200	4	8.06646416329215298902e-17
2240	89	1.89759388814249307931e-08
2268	2	4.03323208164607649451e-17
2304	187	1.46981382817372441263e-07
2340	1	2.01661604082303824725e-17
2352	12	2.62160085306994972143e-16
2376	2	4.03323208164607649451e-17
2400	121	7.68120562294472009057e-09
2464	2	4.03323208164607649451e-17
2496	5	1.00830802041151912363e-16
2520	19	3.83157047756377266978e-16
2560	99	9.52879874516806418816e-08
2592	56	4.48746794497884016195e-10
2640	5	1.00830802041151912363e-16
2688	119	2.46360268030005463702e-08
2700	6	1.20996962449382294835e-16
2720	1	2.01661604082303824725e-17
2800	18	9.85830763810396915048e-11
2816	14	3.9972266664169142647e-10
2880	224	1.57514175023500124784e-08
2912	2	4.03323208164607649451e-17
2940	1	2.01661604082303824725e-17
3000	7	1.41163122857612677308e-16
3024	18	3.62990887348146884506e-16
3040	1	2.01661604082303824725e-17
3072	103	9.33353577474860945928e-08
3120	1	2.01661604082303824725e-17
3136	13	9.7852865133668531783e-11
3168	10	2.01661604082303824725e-16
3200	67	1.13766802092244573297e-08
3240	6	1.20996962449382294835e-16
3328	5	1.00830802041151912363e-16
3360	61	8.18627051996784205201e-11
3456	133	1.13324545385727615265e-08
3520	8	1.6132928326584305978e-16
3528	1	2.01661604082303824725e-17
3584	41	1.46504951935213373337e-08
3600	24	2.22905021263902769491e-11
3640	1	2.01661604082303824725e-17
3696	1	2.01661604082303824725e-17

p	N_w	verified measure
3780	2	4.03323208164607649451e-17
3840	165	3.35846411221672053182e-08
3888	5	1.00830802041151912363e-16
3920	2	4.03323208164607649451e-17
3960	1	2.01661604082303824725e-17
4000	13	1.18540902788177859861e-10
4032	60	1.91539026826725855557e-10
4096	27	2.24732561321123319731e-08
4160	1	2.01661604082303824725e-17
4200	4	8.06646416329215298902e-17
4224	15	4.40836603332606102867e-16
4320	41	6.33671505025079628837e-11
4416	1	2.01661604082303824725e-17
4480	47	4.44286632657331370666e-10
4500	1	2.01661604082303824725e-17
4608	109	2.75429096201380840814e-08
4704	4	8.06646416329215298902e-17
4752	1	2.01661604082303824725e-17
4800	59	4.65015083080458357934e-10
4928	2	4.03323208164607649451e-17
4992	4	8.06646416329215298902e-17
5000	1	2.01661604082303824725e-17
5040	8	1.6132928326584305978e-16
5120	46	1.69437647755659587245e-08
5184	27	3.28448097712541464688e-12
5280	2	4.03323208164607649451e-17
5376	71	1.51430259672825917594e-09
5400	2	4.03323208164607649451e-17
5600	6	1.20996962449382294835e-16
5632	2	4.03323208164607649451e-17
5760	111	1.09496048512902621752e-09
6000	5	1.00830802041151912363e-16
6048	4	8.06646416329215298902e-17
6144	58	1.70946220685863625732e-08
6272	3	6.04984812246911474176e-17
6300	1	2.01661604082303824725e-17
6336	2	4.03323208164607649451e-17
6400	38	6.63067415210272237402e-10
6480	4	8.06646416329215298902e-17
6720	17	3.42824726939916502033e-16
6912	80	8.68082543131407091686e-10
7040	1	2.01661604082303824725e-17
7168	23	9.41381698288390467155e-10
7200	12	2.62160085306994972143e-16
7680	78	3.80943674846943858281e-09
7776	1	2.01661604082303824725e-17
7840	2	4.03323208164607649451e-17
8000	7	1.41163122857612677308e-16
8064	28	4.11358252148941172521e-12
8192	8	4.29929311379292911077e-09
8400	2	4.03323208164607649451e-17
8448	5	1.00830802041151912363e-16
8640	8	1.6132928326584305978e-16
8960	14	2.82326245715225354616e-16
9216	63	2.5629170070928797287e-09
9408	2	4.03323208164607649451e-17
9600	23	4.30581091614978817006e-12
10080	1	2.01661604082303824725e-17
10240	30	2.16034582193810886785e-09

p	N_w	verified measure
10368	5	1.00830802041151912363e-16
10752	25	5.8277964702299622779e-11
11200	1	2.01661604082303824725e-17
11264	1	2.01661604082303824725e-17
11520	50	3.45301736422859439912e-11
12288	25	2.52287638046258533286e-09
12544	1	2.01661604082303824725e-17
12800	7	1.6132928326584305978e-16
13440	5	1.00830802041151912363e-16
13824	30	3.00239722406808740018e-11
14336	7	3.0324076799939647664e-11
15360	30	1.3809309164919403301e-10
16000	1	2.01661604082303824725e-17
16128	2	4.03323208164607649451e-17
16384	2	4.58952424241959588969e-10
17280	1	2.01661604082303824725e-17
17920	7	1.41163122857612677308e-16
18432	19	7.0838524282579307112e-11
19200	1	2.01661604082303824725e-17
20480	6	1.48670596666899967886e-10
21504	4	8.06646416329215298902e-17
23040	1	2.01661604082303824725e-17
24576	7	1.96098825112206442967e-10
25600	1	2.01661604082303824725e-17
27648	3	6.04984812246911474176e-17
28672	2	4.03323208164607649451e-17

Table 3: The lower bound of the total stability measure of windows with respect to the principal period p. Also the number of detected windows N_w is given. This means that we found N_w *distinct* orbits of principal period p. The total number of verified sinks is 4970355.